Available online at www.sciencedirect.com
ScienceDirect
Comput. Methods Appl. Mech. Engrg. 336 (2018) 578–593
Computer methods in applied mechanics and engineering
www.elsevier.com/locate/cma

Uncertainty quantification guided robust design for nanoparticles' morphology

Y. He[a,*], M. Razi[b], C. Forestiere[c], L. Dal Negro[d], R.M. Kirby[b]

[a] Department of Mathematics, New Mexico Institute of Mining and Technology, USA
[b] Scientific Computing and Imaging Institute, University of Utah, USA
[c] Department of Electrical Engineering and Information Technology, Università degli Studi di Napoli Federico II, Italy
[d] Department of Electrical and Computer Engineering and Photonics Center, Division of Material Science and Engineering, and Department of Physics, Boston University, USA

Received 3 November 2017; received in revised form 15 March 2018; accepted 19 March 2018
Available online 28 March 2018

Abstract

The automatic inverse design of three-dimensional plasmonic nanoparticles enables scientists and engineers to explore a wide design space and to maximize a device's performance. However, due to the large uncertainty in the nanofabrication process, we may not be able to obtain a deterministic value of the objective, and the objective may vary dramatically with respect to a small variation in uncertain parameters. Therefore, we take into account the uncertainty in simulations and adopt a classical robust design model for a robust design. In addition, we propose an efficient numerical procedure for the robust design to reduce the computational cost of the process caused by the consideration of the uncertainty. Specifically, we use a global sensitivity analysis method to identify the important random variables and consider the non-important ones as deterministic, and consequently reduce the dimension of the stochastic space. In addition, we apply the generalized polynomial chaos expansion method for constructing computationally cheaper surrogate models to approximate and replace the full simulations. This efficient robust design procedure is performed by varying the particles' material among the most commonly used plasmonic materials such as gold, silver, and aluminum, to obtain different robust optimal shapes for the best enhancement of electric fields.

Keywords: Robust design; Uncertainty; Field enhancement; Metal nanoparticles; Sensitivity analysis; Generalized polynomial chaos expansion

1. Introduction

The electromagnetic design of nanostructures has traditionally been carried out without relying on an automatic optimization procedure, resulting in a significant limitation of the accessible design space and of the achievable performance. The recent advances in computational electromagnetic methods and nanofabrication techniques that are

* Correspondence to: 240 Weir Hall, 801 Leroy Place, Department of Mathematics, New Mexico Institute of Mining and Technology, Socorro, NM 87801, USA.
E-mail addresses: yanyan.he@nmt.edu (Y. He), manirazi@sci.utah.edu (M. Razi), carlo.forestiere@unina.it (C. Forestiere), dalnegro@bu.edu (L. Dal Negro), kirby@sci.utah.edu (R.M. Kirby).

https://doi.org/10.1016/j.cma.2018.03.027
0045-7825/

capable of reproducing the nanoconstructs resulting from the numerical design process have triggered the introduction of more rigorous design strategies [1–3]. For example, Liu et al. considered the optimal design of a particular class of nanophotonic structures – an extremely compact photonic-crystal-based wavelength division multiplexer – using finite-element tearing and interconnecting (FETI) method [2]; and Ruan and Fan designed a subwavelength superscattering nanosphere with plasmonic–dielectric–plasmonic layer structure to achieve an enhanced scattering cross section [3]. Additionally Yelk et al. developed optimal design of a 2D symmetric silver lens that focuses an incidence plane wave onto pre-specified, spatially confined spot [1].

Specifically, deterministic inverse design methods have been proposed to design the geometry of metallic nanoparticles which maximize the quantity of interest [4–7]. The authors in Refs. [4,5] obtained an optimal infinite plasmonic cylinder using a full-retarded 2D boundary-element method solver to map the shape parameters to the output and Gielis' superformula to describe the cross section of the cylinder. Feichtner et al. [6] utilized 3D finite-difference-time-domain (FDTD) method to design the optimal 3D plasmonic nanoantenna that consists of a checkerboard of 20×20 discrete gold cubes with 10 nm edge. Forestiere et al. [7] proposed a deterministic inverse design, which involves the parameterization of the morphology of arbitrary 3D particles using Gielis' superformula [8,9], a full-retarded electromagnetic solver based on the surface integral equation method that maps the design parameters to the quantity of interest [10], and an efficient optimization algorithm. The automation of the rigorous inverse-design strategy for the plasmonic design makes it possible to search in a quite large space of 3D shapes, and consequently for the user to obtain a specific nanostructure that meets specific needs.

However, the deterministic design strategies mentioned above are normally based on the simulation/modeling of the physical process and the nanofabrication of the designed structure, which inevitably involve uncertainty. Without considering the uncertainties in the simulations and/or the nanofabrication process, the deterministic strategy may lead to non-robust designs. To resolve this issue, robust optimal design model has been utilized to take into account the uncertainty in the system for a robust design, where the best compromise between high performance and low uncertainty is obtained. The uncertainties in the engineering systems are usually characterized by random parameters in the framework of probability theory, and a classical robust model aims to optimize the mean system response while minimizing its variability (standard deviation) [11–13].

The optimization process under uncertainty requires the evaluation of mean and standard deviation of the cost function for any specific design in the search space. Traditionally, the Monte Carlo (MC) sampling method (which implements the simulations at the drawn samples based on the distribution of the random inputs and obtains the corresponding samples for the model output) is applied for the estimation of the statistical moments of the cost function. MC method is easy to understand and implement. However, due to its slow convergence, it may require a large number of evaluations of the full simulation model to achieve the desired accuracy in the statistical quantities of interest. Therefore, the MC method could be viewed as being robust at the expense of being numerically expensive.

To represent the uncertainty in the output and calculate the mean and standard deviation more efficiently, we adopt the generalized polynomial chaos (gPC) expansion method to construct a computationally cheaper surrogate to approximate the full simulation models. The gPC method can be used to expand any square integrable random function in the stochastic space in terms of orthogonal polynomials of the random variable. Initially, Hermite polynomials are used for functions with Gaussian distributed random inputs based on the homogeneous chaos theory [14], then extends to different types of orthogonal polynomials in the Askey scheme corresponding to different types random variables [15]. By matching the probability density function (PDF) of random variables to the weighting function of orthogonal polynomials, the gPC expansion with this specific type of polynomial basis is capable of converging rapidly to a smooth function. The convergence rate of the gPC expansion relies on the smoothness of the function, measured by its differentiability. With other types of polynomials as the basis of gPC expansion, one can still obtain a convergent series at the cost of inducing larger approximation errors and a more complex gPC representation [16]. In the current work, we use Legendre polynomials for variables with uniform distribution and Hermite polynomials for Gaussian distribution based on the Askey scheme. In addition, we adopt a discrete projection method [17] to calculate the gPC coefficients, which is a non-intrusive method treating the simulation code as a black box.

The construction of a gPC expansion is efficient for low-dimensional problems; however, it may become expensive when the stochastic space dimension is large. In this case, we implement sensitivity analysis (SA) to identify the "important" uncertain variables. Exploiting the sensitivity analysis, the complexity of the problem can be reduced by considering the non-important variable deterministic. The SA methods can be broadly categorized into two types: local sensitivity analysis and global sensitivity analysis. There may be different interpretations on "local" and "global"

for sensitivity analysis in the literature. However, in the current work, we follow the reference [18] where the local sensitivity analysis investigates the impact on the model output based on the small perturbations of input variables only very close to a fixed point (normally with the nominal values), and the local sensitivity is measured using partial derivatives evaluated at the fixed point in the space of input. On the other hand, global sensitivity analysis explores the impact on the model output based on the uncertainty of the input variables over the whole parametric space. When the stochastic space of input parameters is large, the uncertainty cannot be considered as the small perturbations very close to the nominal values, consequently local sensitivity analysis may not be proper for the use of identifying the "important" parameters. Therefore, we focus on global sensitivity analysis in the current work. The procedure involves the simulation runs to map the model output from the uncertain input, and the calculation of the sensitivity measures. There are different indices to measure global sensitivity in the literature, and they perform differently for different types of mathematical models. For example, Standardized Regression Coefficients (SRC) works well for linear functions; the measures based on rank transforms such as Partial Rank Correlation Coefficient (PRCC) work well for nonlinear but monotonic relationships between outputs and inputs [18]. For nonlinear non-monotonic function, variance-based SA measures such as Sobol indices are the best choice [19]. Since the electromagnetic model has clearly shown the non-monotonic trend with respect to the shape parameters in our previous work [7], we adopt Sobol indices as global SA measure here. The Sobol indices can be calculated using Monte Carlo sampling method [20]. Again, due to the slow convergence, one may need to run large number of electromagnetic simulations to reach a reasonable result, which could be computational expensive or even infeasible. Therefore we implement the calculation of Sobol indices based on gPC expansion [21]. By comparing the value of Sobol indices, we are able to identify the "important" uncertain variables and possibly reduce the dimension of stochastic space.

This paper is organized as follows. In Section 2, we introduce the background on the deterministic inverse design for nanoparticles, general polynomial chaos expansion method and global sensitivity analysis for Sobol indices calculation. Following that, we propose an efficient numerical method for robust design of metal nanoparticles and provide a simple one-dimensional example as an illustration in Section 3. In Section 4, the proposed numerical strategy is applied to the robust design of nanoparticles with different materials. A summary is provided in Section 5.

2. Background

2.1. Deterministic inverse design

In our previous work [7], the deterministic inverse design has been formulated for the monochromatic linear electromagnetic scattering by a single homogeneous and isotropic nanoparticle. The objective was to design the optimal surface morphology Σ of a specific metal nanoparticle, which is excited by the external field at a specific wavelength λ, so that the best desired performance of the design is achieved.

To implement the optimization mathematically, the surface morphology Σ of the nanoparticles has been parameterized and represented in mathematical form based on Gielis' superformula. Gielis' superformula is a generalization of superellipses formula. By relaxing the constraints of superellipses, Gielis' superformula is capable of describing a large set of shapes in nature. The 3D formula is provided in [7] and the following.

$$\begin{aligned} x &= \eta\, r_1(\phi)\cos(\phi)\, r_2(\theta)\cos(\theta) \\ y &= \eta\, r_1(\phi)\sin(\phi)\, r_2(\theta)\cos(\theta) \\ z &= \eta\, r_2(\theta)\sin(\theta) \end{aligned} \tag{1}$$

where

$$\begin{aligned} r_1(\phi) &= \left[\left|\frac{\cos\left(\frac{m^{(\phi)}}{4}\phi\right)}{a^{(\phi)}}\right|^{n_2^{(\phi)}} + \left|\frac{\sin\left(\frac{m^{(\phi)}}{4}\phi\right)}{b^{(\phi)}}\right|^{n_3^{(\phi)}}\right]^{\frac{1}{n_1^{(\phi)}}} \\ r_2(\theta) &= \left[\left|\frac{\cos\left(\frac{m^{(\theta)}}{4}\theta\right)}{a^{(\theta)}}\right|^{n_2^{(\theta)}} + \left|\frac{\sin\left(\frac{m^{(\theta)}}{4}\theta\right)}{b^{(\theta)}}\right|^{n_3^{(\theta)}}\right]^{\frac{1}{n_1^{(\theta)}}} \end{aligned} \tag{2}$$

and $\theta \in [0, \pi]$, $\phi \in [0, 2\pi]$.

As described in [8,7], the parameter η controls the scaling of the resulting shape; and the parameters m, n_1, n_2, n_3, a, and b with the superscript (ϕ) control the shape variation along the azimuthal angle ϕ, while those with the superscript (θ) describe the shape along the altitude angle θ (zenith). Specifically, m indicates the number of sections to which the plane is divided, instead of the fixed four sections or quadrants as in the superellipses; a and b controls how elongated the shape is, which is similar as in the case of superellipses; n_2 and n_3 determine whether the shape is inscribed or circumscribed in the unit circle.

The surface morphology can be completely described by thirteen parameters based on the superformula. However, we keep fixed the altitude parameters in [7] since we are interested in shapes compatible with *planar* nano-fabrication technology:

$$m^{(\theta)} = 2; \qquad n_i^{\theta} = 2 \quad \forall i = 1, 2, 3; \qquad a^{(\theta)} = b^{(\theta)} = 1. \tag{3}$$

We also bound the following azimuthal parameters to exclude the shapes with extremely sharp edges in the searching space:

$$1 \leq m^{(\phi)} \leq 8; \qquad 0.75 \leq n_i^{(\phi)} \leq 6 \quad \forall i = 1, 2, 3; \qquad 0.25 \leq a^{(\phi)}, b^{(\phi)} \leq 2. \tag{4}$$

Furthermore, the scaling factor η is also constrained in order to avoid excessively small or large particles:

$$25 \cdot 10^{-9} \leq \eta \leq 75 \cdot 10^{-9}. \tag{5}$$

In the current work, we make the same assumptions on the parameters of the superformula. Therefore, the surface of a nanoparticle Σ is fully parameterized by the shape parameters $\Gamma = \{m^{(\phi)}, n_1^{(\phi)}, n_2^{(\phi)}, n_3^{(\phi)}, a^{(\phi)}, b^{(\phi)}\}$, and the design space is the seven-dimensional space of the azimuthal parameters and scaling factor of the shape.

Similarly as in the previous work [7], our desired performance of a metallic nanoparticle is considered in terms of the averaged electric-field enhancement on the surface of particle, which is calculated using the electromagnetic solver — Electromagnetic Surface Integral Equations (SIE). Let Σ denote the particle's surface, which divide the entire electromagnetic field domain $\mathbb{R}^3$ into the interior of the dielectric domain $\Omega^{(i)}$ and the external medium $\Omega^{(e)}$. Correspondingly, let ϵ_i and ϵ_e denote the linear permittivity of the particle and of the embedding medium. Specifically, we set ϵ_i equal to that of real world metals such as gold, silver, or aluminum, and ϵ_e to be the permittivity of air ϵ_0. In addition, the external electric and magnetic fields at wavelength λ are denoted as $(\mathbf{E}_0, \mathbf{H}_0)$, and total fields are denoted with $\left(\mathbf{E}^{(i)}, \mathbf{H}^{(i)}\right)$ and $\left(\mathbf{E}^{(e)}, \mathbf{H}^{(e)}\right)$ in $\Omega^{(i)}$ and $\Omega^{(e)}$, respectively. Then the scattered fields $\left(\mathbf{E}_S^{(i)}, \mathbf{H}_S^{(i)}\right)$ and $\left(\mathbf{E}_S^{(e)}, \mathbf{H}_S^{(e)}\right)$ can be defined as:

$$\begin{matrix} \mathbf{E}_S^{(i)} = \mathbf{E}^{(i)} \\ \mathbf{H}_S^{(i)} = \mathbf{H}^{(i)} \end{matrix} \; in\ \Omega^{(i)}; \qquad \begin{matrix} \mathbf{E}_S^{(e)} = \mathbf{E}^{(e)} - \mathbf{E}_0 \\ \mathbf{H}_S^{(e)} = \mathbf{H}^{(e)} - \mathbf{H}_0 \end{matrix} \; in\ \Omega^{(e)}, \tag{6}$$

which satisfies the Maxwell's equations

$$\nabla \times \mathbf{E}_S^{(t)} = -j\omega\mu_0 \mathbf{H}_S^{(t)}, \qquad \nabla \times \mathbf{H}_S^{(t)} = j\omega\varepsilon_t \mathbf{E}_S^{(t)} \quad \text{in } \Omega^{(t)}, \quad \text{with } t = i, e; \tag{7}$$

with boundary conditions

$$\mathbf{n} \times \left(\mathbf{H}_S^{(e)} - \mathbf{H}_S^{(i)}\right) = -\mathbf{n} \times \mathbf{H}_0; \qquad \mathbf{n} \times \left(\mathbf{E}_S^{(e)} - \mathbf{E}_S^{(i)}\right) = -\mathbf{n} \times \mathbf{E}_0 \quad \text{on } \Sigma \tag{8}$$

where a time-harmonic dependence $e^{j\omega t}$ has been assumed and j is the imaginary unit. The equations are solved with the radiation condition at infinity.

With a fixed excitation wavelength of the external field, the average field enhancement on the surface Σ is calculated as

$$g(\Gamma) = \frac{1}{\Sigma(\Gamma)} \iint_{\Sigma(\Gamma)} \left\| \frac{\mathbf{E}^{(e)}}{\mathbf{E}_0} \right\| dS. \tag{9}$$

As mentioned earlier, the objective of deterministic inverse design is to maximize the average field enhancement g with respect to the set of shape parameters $\Gamma = \{m^{(\phi)}, n_1^{(\phi)}, n_2^{(\phi)}, n_3^{(\phi)}, a^{(\phi)}, b^{(\phi)}\}$ of the nanoparticles. However, the optimal deterministic design may fail due to the uncertainty in the simulation process. Therefore, we quantify the uncertainty in the system using the generalized Polynomial Chaos expansion method and implement robust design under uncertainty.

2.2. Stochastic uncertainty propagation using polynomial chaos expansion

In the current work, we assume that the uncertainty in the system is represented using random variables, and introduce the basics of the generalized Polynomial Chaos (gPC) expansion for stochastic uncertainty propagation in this section.

First we represent a complete probability space using a triplet $(\Omega, \mathcal{F}, \mathcal{P})$, where the sample space Ω is the set of all possible outcomes, $\mathcal{F} \subset 2^{\Omega}$ is the σ-algebra collecting all measurable events that belongs to Ω, and $\mathcal{P} : \mathcal{F} \to [0, 1]$ is the probability measure indicating each event's likelihood of occurrence. Let $\boldsymbol{\xi} = \{\xi_1(\omega), \xi_2(\omega), \ldots, \xi_n(\omega)\} : \Omega \to \Xi \subseteq \mathcal{R}^n$ be a set of uncorrelated random variables, which represent the uncertainty in the system. Then any second-order random variables $u(\omega) \in \mathbf{L}_2(\Omega, \mathcal{P})$ (i.e., $\langle u, u\rangle = \|u\|^2_{\Omega} < \infty$) can be represented as follows [22,23,15]:

$$u(\boldsymbol{\xi}(\omega)) = \sum_{i=0}^{\infty} \hat{u}_i \, \Phi_i(\boldsymbol{\xi}(\omega)), \tag{10}$$

where the functions Φ_i were originally proposed as Wiener–Hermite polynomial chaos (with the assumption of $\boldsymbol{\xi}$ having Gaussian distribution) by Wiener [14] and later extended to the generalized polynomial chaos (more classical orthogonal polynomials) via the Askey scheme. The choice of the type of the polynomial chaos depends on the distribution of the random inputs. In the current work, we adopt Hermite polynomials for Gaussian random variables and Legendre polynomials for uniform random variables; and the parameters $\hat{u}_i$s are called the gPC coefficients.

For the purpose of numerical calculation, the series is usually truncated up to polynomial order p with N terms ($N = \frac{(n+p)!}{n!p!}$) to approximate the exact output $u(\boldsymbol{\xi}(\omega))$

$$u_p(\boldsymbol{\xi}(\omega)) = \sum_{i=0}^{N-1} u_i \, \Phi_i(\boldsymbol{\xi}(\omega)). \tag{11}$$

Based on the orthogonality of the polynomial basis, the gPC coefficients can be calculated by projecting u on each basis using the inner product

$$u_i = \frac{\langle u, \Phi_i\rangle}{\langle \Phi_i, \Phi_i\rangle} = \frac{1}{E[\Phi_i^2]} \int_{\Xi} u(\boldsymbol{\xi}) \Phi_i(\boldsymbol{\xi}) \rho(\boldsymbol{\xi}) d\boldsymbol{\xi}, \tag{12}$$

where $\rho(\boldsymbol{\xi})$ is the probability distribution of the variable $\boldsymbol{\xi}$, and the integration can be estimated using a quadrature rule as

$$u_i \approx \hat{u}_i = \frac{1}{E[\Phi_i^2]} \sum_{j=1}^{M} u(\boldsymbol{\xi}^j) \Phi_i(\boldsymbol{\xi}^j) \alpha^j, \qquad i = 0, 1, \ldots, N-1, \tag{13}$$

where $\{\boldsymbol{\xi}^j, \alpha^j\}_{j=1}^{M}$ is a set of quadrature points and the corresponding weights. The use of tensor product quadrature may have significant efficiency for low-dimensional problems, however, it suffers from the "curse of dimensionality" for high-dimensional cases since the number of quadrature points increases exponentially as the dimension increases. In the current work, we use sparse grid quadrature points [24,25].

Once an accurate gPC expansion $u_p(\boldsymbol{\xi})$ is constructed to approximate the random function $u(\boldsymbol{\xi})$, one has in fact an analytical representation of the function u in terms of $\boldsymbol{\xi}$. Therefore, all the statistical information of u can be retrieved from the gPC expansion in a straightforward manner using their definitions directly. The mth moment of u for $m \in \mathbf{N}$ is

$$E[(u - E[u])^m] \approx E[(u_p - E[u_p])^m] = \int_{-\infty}^{\infty} (u_p(\boldsymbol{\xi}) - E[u_p])^m \rho(\boldsymbol{\xi}) d\boldsymbol{\xi}, \tag{14}$$

which can be calculated either analytically or with small computational effort [16]. In particular, the first and second moments of u can be obtained from the coefficients of gPC expansion directly as follows. The expectation of u only depends on the first coefficient as

$$E[u] \approx E[u_p] \approx \sum_{i=0}^{N-1} \hat{u}_i \langle \Phi_0, \Phi_i\rangle = \hat{u}_0 \langle \Phi_0, \Phi_0\rangle. \tag{15}$$

The variance σ_u^2 is obtained as a weighted sum of its squared gPC coefficients:

$$\sigma_u^2 \approx \sigma_{u_p}^2 = E[(u_p - E[u_p])^2] \approx \sum_{i=1}^{N-1} \hat{u}_i^2 \langle \Phi_i, \Phi_i \rangle. \tag{16}$$

With generalized Polynomial Chaos expansion method, we would be able to quantify the uncertainty in our quantity of interest g (propagated from the uncertainty in the inputs) efficiently using its stochastic moments. The approximation of stochastic moments based on gPC expansion has fast convergency to the truth for smooth functions. However, to evaluate the gPC coefficients accurately, a large number of function evaluations are required and the number increases dramatically with the increase of dimension of the problem. To reduce the computational cost, we implement sensitivity analysis to identify the "important" uncertain variables. Based on which the complexity of the problem can be reduced by considering the non-important variable deterministic.

2.3. Sensitivity analysis

As mentioned in the introduction, sensitivity analysis provides the information on that which specific variation or the combination of the variations plays the most important roles in the quantify of interest of the simulation model. Here we introduce the global sensitivity analysis tool and provide the calculation formula for Sobol indices [19–21].

The Sobol sensitivity indices are calculated based on the ANOVA (analysis of variance) decomposition of a function $u(\boldsymbol{\xi})$ as given in [19,20]:

$$u(\boldsymbol{\xi}) = u_0 + \sum_i u_i(\xi_i) + \sum_{i<j} u_{ij}(\xi_i, \xi_j) + \cdots + u_{1,\ldots,n}(\xi_1, \xi_2, \ldots, \xi_n).$$

where

$$\int u(\boldsymbol{\xi}) d\boldsymbol{\xi} = u_0, \quad \int u(\boldsymbol{\xi}) \Pi_{k\neq i} d\xi_k = u_0 + u_i(\xi_i),$$
$$\int u(\boldsymbol{\xi}) \Pi_{k\neq i,j} d\xi_k = u_0 + u_i(\xi_i) + u_j(\xi_j) + u_{i,j}(\xi_i, \xi_j),$$

and so on.

Based on the decomposition, the so called variance of $u_{i_1,i_2,\ldots,i_r}$ is defined as

$$D_{i_1,i_2,\ldots,i_r} = \int u^2_{i_1,i_2,\ldots,i_r} d\xi_{i_1,i_2,\ldots,i_r},$$

and the total variance is

$$D = \int u^2(\boldsymbol{\xi}) d\boldsymbol{\xi} - u_0^2 = \sum_{r=1}^{n} \sum_{i_1<\cdots<i_r}^{n} D_{i_1,i_2,\ldots,i_r}. \tag{17}$$

Then the global sensitivity indices (called Sobol indices) are defined as

$$S_{i_1,i_2,\ldots,i_r} = D_{i_1,i_2,\ldots,i_r}/D, \tag{18}$$

which can help to rank the "importance" of the variables and consequently fix the unessential variables as deterministic.

The simplest sensitivity indices are the first order Sobol indices

$$S_i = D_i/D, \qquad i = 1, \ldots, n, \tag{19}$$

which measure the sensitivity of the model output (quantity of interest) to each single variable ξ_i alone. One may start with the first order Sobol indices for ranking the "importance" of variables due to its simplicity. However, if the results for the first order indices show that the majority of the output variance is due to interaction effects among factors, the total Sobol indices represent a more meaningful measure to deal with models with such a high nonadditivity [26]. The definition for total indices S_i^{tot} is the sum indices over all the subsets I with $i \in I$.

$$S_i^{tot} = \sum_{I\cap\{i\}\neq\emptyset} S_I, \qquad i = 1, \ldots, n. \tag{20}$$

Numerically, the Sobol indices can be calculated using the Monte Carlo sampling method. However, due to its slow convergence, one may need to run a large number of electromagnetic simulations to reach a reasonable result, which could be computationally expensive or even infeasible. Here we introduce the calculation of Sobol indices based on a gPC expansion.

Let the obtained gPC expansion be

$$u(\boldsymbol{\xi}) \approx \sum_{i=0}^{N-1} \hat{u}_i \, \Phi_i(\boldsymbol{\xi}). \tag{21}$$

Each multivariate polynomial Φ_i can be represented by means of multiple index $\boldsymbol{\alpha} = (\alpha_1, \ldots, \alpha_n)$ as

$$\Phi_i(\boldsymbol{\xi}) = \Phi_{\boldsymbol{\alpha}} = \Pi_{i=1}^{n} \phi_{\alpha_i}(\xi_i), \tag{22}$$

where $\phi_{\alpha_i}(\xi_i)$ is the one-dimensional α_ith polynomial. Let $\mathcal{I}_{\{i_1,\ldots,i_r\}}$ be the set of $\boldsymbol{\alpha}$ multi-indices where only $\alpha_k \neq 0$ for $k = i_1, i_2, \ldots, i_r$. Then the gPC expansion can be rewritten as

$$u(\boldsymbol{\xi}) \approx \sum_{s=1}^{n} \sum_{\alpha \in \mathcal{I}_{\{i_1,\ldots,i_r\}}} \hat{u}_\alpha \, \Phi_\alpha(\xi_{i_1}, \ldots, \xi_{i_s}). \tag{23}$$

Following that, the Sobol indices are approximated by,

$$S_{i_1,i_2,\ldots,i_r} = \frac{1}{D} \sum_{\alpha \in \mathcal{I}_{\{i_1,\ldots,i_r\}}} \hat{u}_\alpha^2 \int \Phi_\alpha^2(\boldsymbol{\xi}) \rho(\boldsymbol{\xi}) d\boldsymbol{\xi}, \tag{24}$$

where,

$$D = \sum_{i=1}^{N-1} \hat{u}_i^2 \int \Phi_i^2(\boldsymbol{\xi}) \rho(\boldsymbol{\xi}) d\boldsymbol{\xi}. \tag{25}$$

With the calculated Sobol indices that indicate how sensitive the quantity of interest g is with respect to the variation of the shape parameters, one can rank the importance of the uncertain variables. Based on the ranking, the non-important uncertain variables are considered as deterministic, and consequently, the complexity of the problem is reduced due to the dimension reduction of the stochastic space.

Next, we propose the numerical method for robust inverse design under uncertainty for the plasmonic device. The goal is to obtain a designed geometry for 3D nanoparticle so that its desired property is optimal with respect to other geometries and robust with respect to small structural fluctuations.

3. Numerical method for robust optimization

3.1. Problem setup for robust inverse design under uncertainty

Due to the uncertainty in the design process, such as the errors in the nanofabrication process, we may not be able to obtain a deterministic value of the objective — average field enhancement, not to mention maximize the objective with respect to the design parameters. Instead, our goal is to take into account the uncertainty in the simulation process and maximize the expected value of the objective function.

In addition, the design may not be robust due to the uncertainty in the system, i.e., the objective may vary dramatically with respect to a small variation in uncertain parameters. To resolve this issue, a robust design model is proposed to minimize the standard deviation of the objective function as well as maximizing its expected value.

In the current work, we assume that the uncertainty in the electromagnetic system can be represented using random shape parameters Γ with Gaussian distribution as follows.

$$\begin{aligned} m^{(\phi)} &= \bar{m}^{(\phi)} + \xi_m, \\ n_i^{(\phi)} &= \bar{n}_i^{(\phi)} + \xi_{n_i}, \qquad i = 1, 2, 3 \\ a^{(\phi)} &= \bar{a}^{(\phi)} + \xi_a, \\ b^{(\phi)} &= \bar{b}^{(\phi)} + \xi_b, \\ \eta &= \bar{\eta} + \xi_\eta, \end{aligned}$$

where the mean of design variables $\bar{\Gamma} = \{\bar{m}^{(\phi)}, \bar{n}_i^{(\phi)}, \bar{a}^{(\phi)}, \bar{b}^{(\phi)}, \bar{\eta}\}$ are deterministic, while $\boldsymbol{\xi} = \{\xi_m, \xi_{n_i}, \xi_a, \xi_b, \xi_\eta\}$ is a set of random variables of Gaussian distribution with mean zero. Based on the setup, the design variable becomes $\bar{\Gamma}$ that is deterministic, and the objective function g depends on both design variable and random variable $\boldsymbol{\xi}$.

Due to the randomness of the simulation model input $\Gamma = \{\bar{\Gamma}, \boldsymbol{\xi}\}$, the model output – average field enhancement $g(\Gamma)$ becomes random as well. Consequently, optimizing the (random) objective function for the best deterministic design becomes infeasible. Instead, we adopt the classical robust design model from the references [11–13] to deal with the uncertainty in the model output for a robust design. The objective function of the robust design optimization with respect to the nanoparticles' morphology is formulated as follows.

$$\bar{\Gamma}^* = \underset{\bar{\Gamma}}{\operatorname{argmax}}\, E(g(\Gamma)) - \beta\sigma(g(\Gamma)), \tag{26}$$

where $E(g), \sigma(g)$ are the mean and standard deviation of the objective function. The regularization coefficient $\beta > 0$ is introduced to control the trade-off between the desired objective and the robustness of the design; it reflects the risk attitude of the designer. The larger the value of β is, the designer has more conservative attitude towards uncertainty and the obtained design intends to be more robust. The value of β can be decided empirically based on the specific requirement of the chemists for the designed device. The automatic adaptation of the regularization parameter is beyond the scope of this work.

Sometimes, the robust design model can also be formulated as a constrained optimization problem as

$$\max E(g(\Gamma)), \qquad \text{subject to} \qquad \sigma(g(\Gamma)) \leq TOL, \tag{27}$$

where TOL is the tolerance of the variation on the objective that the electronic device can afford based on the chemists' intuition and experience.

By implementing the robust design model, one can obtain a designed geometry Γ for 3D nanoparticle so that one's objective achieves optimality with respect to other geometries and it is robust with respect to small structural fluctuations.

One needs to calculate the statistics (mean and standard deviation) of the random output many times (for each specific value set of design variables) in order to solve the robust design problem. In addition, each calculation of the statistics requires large number of electromagnetic solver implementations. Therefore, solving the robust design could be computationally expensive. We next present an efficient numerical strategy based on gPC expansion method, which considers the gPC expansion as a surrogate model to replace the full electromagnetic solver. Based on this surrogate model, we approximate the mean value and the standard deviation of the objective function $E(g)$ and $\sigma(g)$, respectively.

3.2. Approximation of statistics of objective function

In this section, we construct a computational cheaper surrogate model to approximate the true function, and consequently calculate the numerical statistics of objective function based on the surrogate to approximate the true ones.

In the current work, the surrogate model is constructed based on gPC expansion method. First, we generate two sets Q_u and Q_g of quadrature points corresponding to variables with uniform distribution and variables with Gaussian distribution, respectively. We then run the electromagnetic solver over the tensor product of two sets (i.e., $(\bar{\Gamma}, \boldsymbol{\xi}) \in Q_u \times Q_g$). Following which, we construct gPC expansion g_p for any fixed value of $\bar{\Gamma} \in Q_u$ over the stochastic space of $\boldsymbol{\xi}$.

$$g_p(\bar{\Gamma}, \boldsymbol{\xi}) = \sum_{i=0}^{N-1} \hat{g}_i(\bar{\Gamma})\Phi_i(\boldsymbol{\xi}), \tag{28}$$

where $\Phi_i(\boldsymbol{\xi})$s are Hermite polynomials, and p is the highest order of the polynomials.

As mentioned in the background, one can estimate the mean and standard deviation using the gPC expansion for each fixed value of $\bar{\Gamma}$ as

$$E[g_p](\bar{\Gamma}) = \hat{g}_0(\bar{\Gamma}), \tag{29}$$

$$\sigma_{g_p}(\bar{\Gamma}) = \sum_{i=1}^{N-1} \hat{g}_i^2(\bar{\Gamma})\langle\Phi_i, \Phi_i\rangle. \tag{30}$$

Next, we construct another gPC expansion over the design space to approximate the mean and standard deviation:

$$E_p(\bar{\Gamma}) = \sum_{i=0}^{N-1} \hat{E}_i \mathbf{L}_i(\bar{\Gamma}), \tag{31}$$

$$\sigma_p^2(\bar{\Gamma}) = \sum_{i=1}^{N-1} \hat{\sigma}_i \mathbf{L}_i(\bar{\Gamma}), \tag{32}$$

where $\mathbf{L_i}$s are Legendre polynomials, and the polynomial order p could be different in gPC expansions of the mean and the standard deviation.

In this work, we use gPC expansion method to construct the surrogates for the function itself and its mean and standard deviation. However, we need to emphasize that the choice of the numerical methods of surrogate construction is in large part a subjective choice, and it does not effect the application of the proposed method so long as the error of the numerical approximation converges to zero as the approximation order approaches to infinity.

Using the surrogate models, the optimization problem for robust design becomes

$$\bar{\Gamma}^* = \underset{\bar{\Gamma}}{\text{argmax}}\, E_p(\bar{\Gamma}) - \beta\sigma_p(\bar{\Gamma}), \tag{33}$$

or the constrained optimization problem

$$\max E_p(\bar{\Gamma}), \qquad \text{subject to} \qquad \sigma_p(\bar{\Gamma}) \leq TOL. \tag{34}$$

Note: With any standard optimization tools, the optimization problem can be solved very efficiently due to the use of the surrogate model. In the current work, we employ one of the most standard algorithms, the quasi-Newton method, to solve all the optimization problems.

Next, a simple one-dimensional example is provided to illustrate the proposed numerical method.

3.3. An example

For the purpose of testing the numerical method, we focus on gold nanoparticles with one uncertain shape parameter and demonstrate the convergence of the numerical approximation of the statistics of the average field enhancement.

3.3.1. Estimation of the mean and standard deviation

We consider gold nanoparticle excited by the plane wave with wavelength $\lambda = 700$ nm. In the deterministic setup provided in previous study [7], the optimal shape for gold nano-particle is the one with the parameters $\Gamma = \{25, 6.10, 3.4, 4.33, 4.25, 2.0, 0.5\}$. To simplify the problem in this illustrative example, we assume that the shape parameters take values around this optimal set. Furthermore, due to the local sensitivity analysis in [7] (see Fig. 1(a)), which shows that the variation of the objective function δ_{g_r} is much larger when the shape parameter $n_1^{(\phi)}$ varies, we consider $n_1^{(\phi)}$ as the only uncertain variable while keep the other shape parameters deterministic as $\eta = 25$, $m^{\{\phi\}} = 6.10$, $n_2^{\{\phi\}} = 4.33$, $n_3^{\{\phi\}} = 4.25$, $a^{\{\phi\}} = 2.0$, $b^{\{\phi\}} = 0.5$. In addition, we set the uncertain variable as $n_1^{(\phi)} = \bar{n}_1^{(\phi)} + \xi_{n_1}$, where $\bar{n}_1^{(\phi)} = 3.4$ and ξ_{n_1} is Gaussian distribution with mean zero and standard deviation 0.1.

Based on the assumptions, the average field enhancement g becomes random and dependent on one random input $n_1^{(\phi)}$ (or ξ_{n_1}). We construct a generalized Polynomial Chaos expansion $g_p(n_1^{(\phi)})$ to approximate the objective function $g(n_1^{(\phi)})$ and consequently estimate its mean and standard deviation. The constructed gPC expansions (g_p versus $n_1^{(\phi)}$) with different highest polynomial order $p = 3, 5, 7$ are shown in Fig. 1(b). As expected, one can observe that the gPC expansion is closer to the truth as the polynomial order is higher. We then calculate the mean $E[g_p]$ and standard deviation σ_{g_p} of the average field enhancement using the surrogate g_p, and analyze their convergence with respect to the polynomial order. The reference values $E[g] = 18.0732$ and $\sigma_g = 2.3051$ are obtained using 100 000 Monte Carlo simulations. The convergence rate of the numerical approximation with respect to p is provided in Fig. 1(c, d) for the mean and standard deviation, respectively. From the figure, one can conclude that the numerical approximations converge to the truth exponentially.

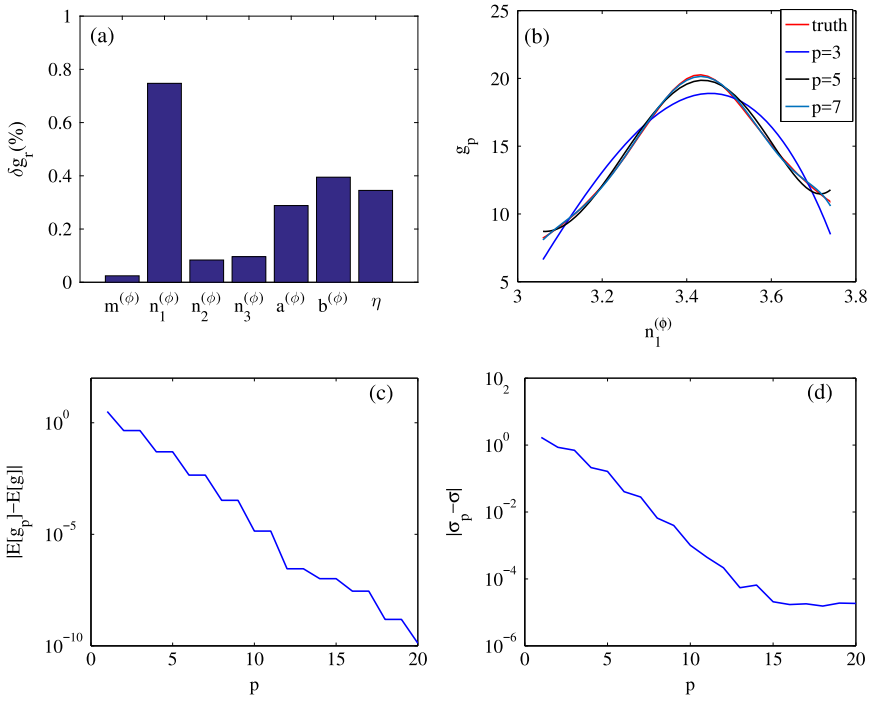

Fig. 1. (a) The variation of the objective function with respect to the variation in each shape parameter; (b) The average field enhancement g_p with respect to the shape parameter $n_1^{(\phi)}$ for different approximation orders; (c) The convergence rate of the mean of average field enhancement with respect to approximation order (i.e., error in $E[g_p]$ versus p); (d) The convergence rate of the standard deviation of average field enhancement with respect to approximation order (i.e., error in σ_{g_p} versus p).

3.3.2. Robust optimization using numerical method

Now we implement robust design for gold nanoparticle. Similarly, we assume $n_1^{(\phi)} = \bar{n}_1^{(\phi)} + \xi_{n_1}$ is the only uncertain parameter, $\xi_{n_1} \sim \mathcal{N}(0, 0.1^2)$ is the random variable. Instead of having a fixed value for $\bar{n}_1^{(\phi)} = 3.4$ as in Section 3.3.1, we consider it as a design variable in the range $[0.75, 6]$ and obtain the robust design using the proposed approach with $\beta = 5.5$. The robust design with $\bar{n}_1^{(\phi)} = 3.561$ is shown in Fig. 2(a) for which the mean is $E = 15.69$ and standard deviation is $\sigma = 1.71$. Compared to design with $\bar{n}_1^{(\phi)} = 3.4$ with mean $E = 15.72$ and $\sigma = 1.89$, the obtained design is more robust (i.e., the objective function variates less with respect to the variations of the shape parameter) with a slight compromise in the mean of the objective function.

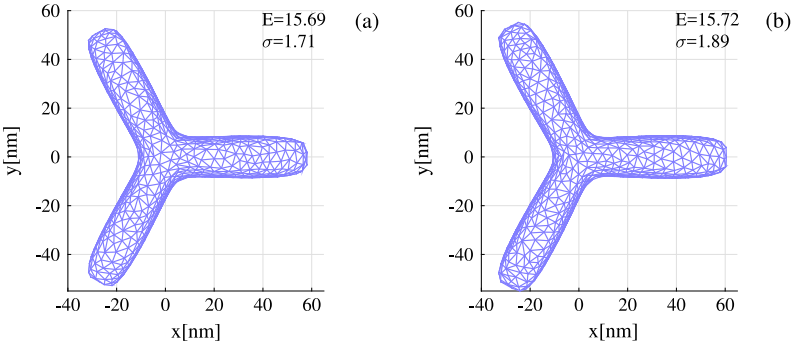

Fig. 2. Optimal design for one-dimensional example: (a) The robust optimal design for gold nanoparticle; (b) the deterministic optimal design.

4. Numerical examples

In this section we implement the proposed efficient numerical method for the robust design of metallic nanoparticles' morphology, which maximizes mean and minimize the standard deviation of the field enhancement when excited by a monochromatic plane-wave of unit intensity, linearly polarized along the x-axis and propagating along the z-axis. In the following, we will present the optimal design for different metal materials, respectively.

4.1. Silver

We first consider the robust optimal design for silver nano particles with the wavelength $\lambda = 400$ nm since the field enhancement reaches the maximum at this wavelength from our previous study [7]. To reduce the computational cost, we implement the global sensitivity analysis to identify the "significant" shape parameters and consider only those as uncertain design variables. The first order Sobol indices for all seven shape parameters are plotted in Fig. 3(left). Since the sum of all first order indices $\sum_i S_i = 0.3849$ is much less than one, indicating the majority of the output variance is due to interaction effects among factors, we also calculate the total Sobol indices and provide the results in Fig. 3(right). One can observe that the most significance shape parameters are $n_1^{(\phi)}$ and η. Therefore, we consider the uncertainty in these two design parameters and define them as $n_1^{(\phi)} = \bar{n}_1^{(\phi)} + \xi_{n_1}$, and $\eta = \bar{\eta} + \xi_\eta$ with $\xi_{n_1} \sim \mathcal{N}(0, 0.1^2)$ and $\xi_\eta \sim \mathcal{N}(0, 1)$. The remaining five design parameters are kept as deterministic as $m^{(\phi)} = 4.38$, $n_2^{(\phi)} = 0.89$, $n_3^{(\phi)} = 6$, $a^{(\phi)} = 1.39$, $b^{(\phi)} = 0.5$.

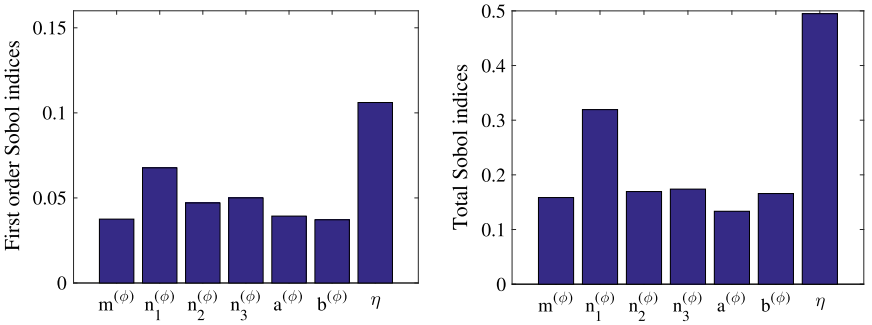

Fig. 3. Sobol indices of shape parameters for silver: (left) the first order indices; and (right) the total indices.

We construct the surrogate model using the gPC method over the four-dimensional space (the tensor product of two-dimensional design space and the two-dimensional stochastic space). The mean and standard deviation of the field enhancement over the stochastic space are calculated and plotted in Fig. 4. The red stars in Fig. 4 (left) are the collocation points with output obtained directly from the full simulation. Based on these collocation points, the response surface for the mean of field enhancement over the two-dimensional design space is constructed using gPC expansion with the collocation points. Fig. 4 (right) shows the response surface of mean ± standard deviation.

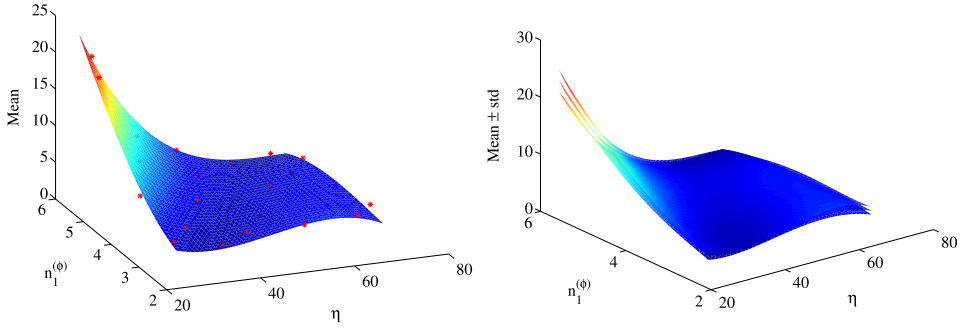

Fig. 4. The numerical approximation of mean (left) and mean ± the standard deviation (right) of the field enhancement.

The robust design with $\bar{n}_1^{(\phi)} = 5.694$ and $\bar{\eta} = 25.0001$ obtained by solving the optimization problem with $\beta = 8$ is provided in Fig. 5. The mean and the standard deviation of the average field enhancement are $E = 19.65$ and

$\sigma = 1.55$. The deterministic optimal parameters obtained in Ref. [7] were $n_1^{(\phi)} = 5.71$ and $\eta = 25$, assigning them to be the values of the design parameter in robust design, we obtain the mean of 19.77 and standard deviation of 1.57. Based on which, one can conclude that with some compromise of the mean of the field enhancement, the robust design is more stable with respect to the uncertainty.

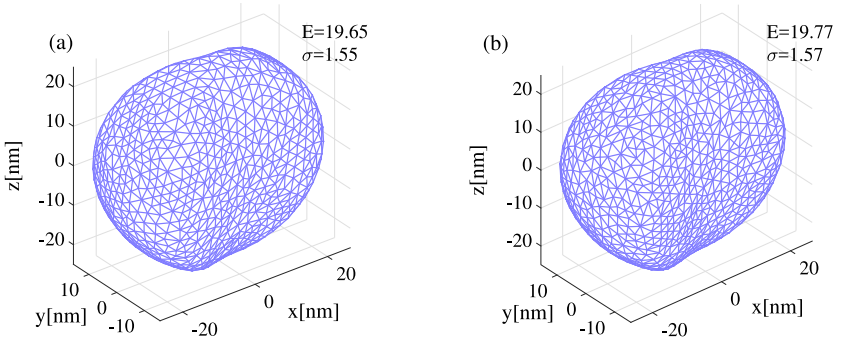

Fig. 5. Optimal design for silver nanoparticle: (a) The robust optimal design; (b) The deterministic optimal design.

4.2. Gold

We then design the robust optimal shape for gold nano particles at the fixed wavelength $\lambda = 700$ nm where the electric field enhancement reaches its maximum [7]. Similarly, we implement the global sensitivity analysis to identify the "important" shape parameters and consider only those as uncertain design variables. In Fig. 6 (left) of the first order Sobol indices, one can observe that the interacting terms have high effects on the model output since the sum of first order indices $\sum_i S_i = 0.2728$ is also much less than one. Therefore, we provide the total Sobol indices in Fig. 6 (right), which shows that the most important shape parameters are $n_2^{(\phi)}$, $a^{(\phi)}$ and $b^{(\phi)}$. Therefore, we only consider the uncertainty in these three design parameters while keeping the other four design parameters fixed as $m^{(\phi)} = 6.10$, $n_1^{(\phi)} = 3.4$, $n_3^{(\phi)} = 4.25$, $\eta = 25$ [7]. The uncertain parameters are defined as $n_2^{(\phi)} = \bar{n}_2^{(\phi)} + \xi_{n_2}$, $a^{(\phi)} = \bar{a}^{(\phi)} + \xi_a$, and $b^{(\phi)} = \bar{b}^{(\phi)} + \xi_b$, where $\xi_{n_2} \sim \mathcal{N}(0, 0.1^2)$ and $\xi_a, \xi_b \sim \mathcal{N}(0, 0.05^2)$.

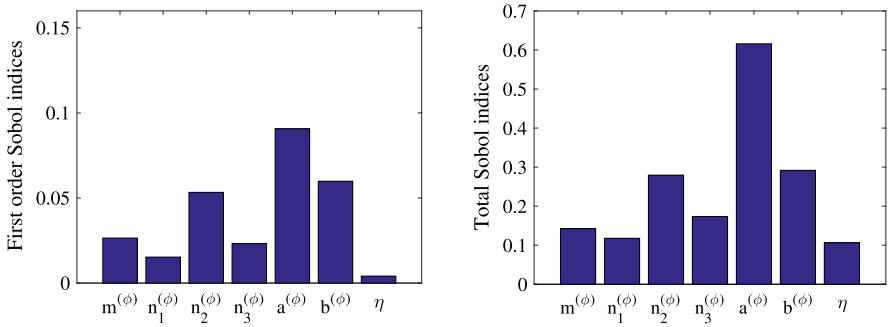

Fig. 6. Sobol indices of shape parameters for gold: (left) the first order indices; and (right) the total indices.

Similarly, the surrogate model is constructed for the quantity of interest using the gPC method over the six-dimensional space (the tensor product of three-dimensional design space and the three-dimensional stochastic space). The mean and standard deviation of the field enhancement are then calculated over the stochastic space.

Using the constructed surrogate for the mean and standard deviation of the field enhancement, we solve the optimization problem with $\beta = 5.5$ to obtain the robust design (see Fig. 7(a)) with $\bar{n}_2^{(\phi)} = 5.8730$, $\bar{a}^{(\phi)} = 2$ and $\bar{b}^{(\phi)} = 1.2365$. The mean and the standard deviation of the average field enhancement are $E = 9.05$ and $\sigma = 1.01$. With the deterministic optimal shape parameters obtained in Ref. [7] as the values for the design parameters, we obtain the mean $E = 11.82$ and standard deviation 2.06. Therefore, one can conclude that with some compromise of the mean of the field enhancement, the robust design is more stable with respect to the uncertainty.

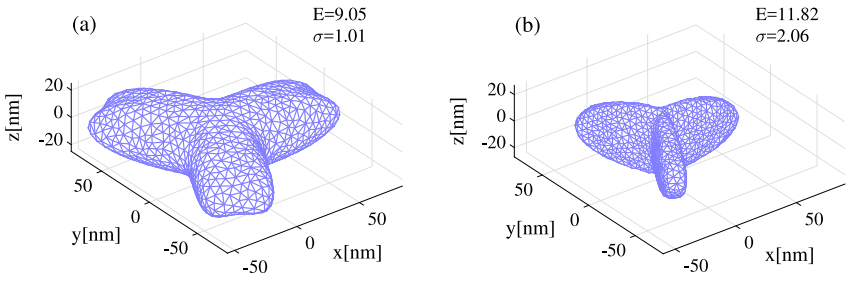

Fig. 7. Optimal design for gold nanoparticle: (a) The robust optimal design; (b) The deterministic optimal design.

4.3. Aluminum

Finally, we consider the robust shape design for aluminum nano particles with the wavelength $\lambda = 150$ nm. Similarly to the design process for the other two types of materials, we implement the global sensitivity analysis to identify the shape parameters to which the quantity of interest is more sensitive. The first order Sobol indices provided in Fig. 8 are used directly to rank the "importance" of parameters since the sum $\sum_i S_i = 0.8244$ is close to one indicating the individual parameter terms have majority of the impact on the model output. The shape parameters $n_1^{(\phi)}$, $n_2^{(\phi)}$, $n_3^{(\phi)}$ and $a^{(\phi)}$ feature the highest Sobol indices and thus are considered as the uncertain design parameters. They are defined as $n_1^{(\phi)} = \bar{n}_1^{(\phi)} + \xi_{n_1}$, $n_2^{(\phi)} = \bar{n}_2^{(\phi)} + \xi_{n_2}$, $n_3^{(\phi)} = \bar{n}_3^{(\phi)} + \xi_{n_3}$, and $a^{(\phi)} = \bar{a}^{(\phi)} + \xi_a$. As discussed in Section 3, the parameter ξ is assumed to be random variables with Gaussian distribution. Based on the magnitude of the design parameters, we further assume $\xi_{n_i} \sim \mathcal{N}(0, 0.1^2)$ $(i = 1, 2, 3)$ and $\xi_a \sim \mathcal{N}(0, 0.05^2)$. The remaining three design parameters are considered as deterministic and their values are assigned as $m^{(\phi)} = 4.10$, $b^{(\phi)} = 0.5$, $\eta = 25$.

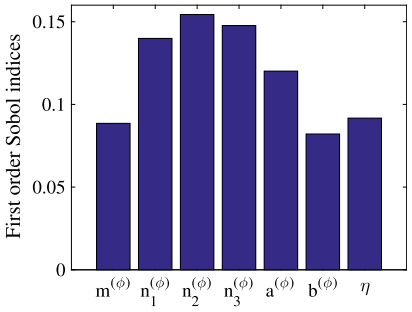

Fig. 8. The Sobol indices of shape parameters for aluminum.

Again, we construct the surrogate model using gPC method over the eight-dimensional space (the tensor product of four-dimensional design space and the four-dimensional stochastic space). Using the gPC expansion, the mean and standard deviation of the field enhancement over the stochastic space are calculated. We then solve the optimization problem with $\beta = 5.5$ for the robust design. The resulting optimal shape is provided in Fig. 9(a). The optimal values of the parameters obtained from the robust design are $\bar{n}_1^{(\phi)} = 2.5$, $\bar{n}_2^{(\phi)} = 2.99$, $\bar{n}_3^{(\phi)} = 3.82$, $\bar{a}^{(\phi)} = 0.53$, and the mean and the standard deviation of the average field enhancement on the surface of the robust design are $E = 7.803$ and $\sigma = 1.44$. On the contrary the deterministic optimal design returned the parameters $\bar{n}_1^{(\phi)} = 1.84$, $\bar{n}_2^{(\phi)} = 2.73$, $\bar{n}_3^{(\phi)} = 3.57$, $\bar{a}^{(\phi)} = 0.5$ with mean $E = 9.111$ and standard deviation $\sigma = 2.11$. Based which, one can draw the same conclusion of a better stability of the robust design.

4.4. Robust design for multiple wavelengths

We are also interested in the robust design for nanoparticles excited by a monochromatic plane-wave of unit intensity with different wavelength λ. Due to the limitation of computational resources, we only focus on silver with the wavelengths $\lambda = 250, 287, 320, 379, 435$ nm as examples. With the same assumption on the uncertainty

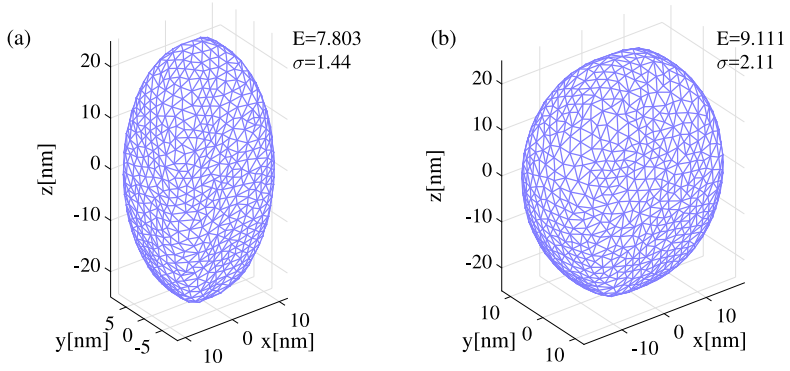

Fig. 9. The robust optimal design for gold nanoparticles to achieve high field enhancement.

in shape parameters as the one in Section 4.1, only two shape parameters $n_1^{(\phi)}$ and η are considered as uncertain. Similarly, we implement the robust optimal design with $\beta = 5.5$ for each wavelength based on the constructed gPC expansion surrogate. The obtained robust designs and the corresponding means and variances of the field enhancement are provided in Table 1.

Table 1
The design shape parameters and the corresponding mean and standard deviation with respect to different wavelengths λ.

λ	$\bar{n}_1^{(\phi)}$	$\bar{\eta}$	E_g	σ_g
250 nm	2.5	25	1.51	0.16
287 nm	2.5	27.4	1.39	0.10
320 nm	2.5	25.1	1.59	0.14
379 nm	5.8	25	7.41	0.94
435 nm	2.7	25	23.76	1.39

The shapes of the robust design are provided in Fig. 10(a–e). Clearly, the robust designs are different for different wavelengths. In the situation where one has control on the wavelength λ at which the metal nanoparticles are excited by the external field, the "ideal" design would be the robust one shown in Fig. 10(e) with specified wavelength $\lambda = 435$ nm since it produces a much higher mean value of field enhancement $E = 23.76$ with a slight compromise on robustness. However, if one cannot specify a fixed wavelength but only its range, the intuitive way would be to consider the average of the field enhancement $\bar{g}$ over the whole range of wavelengths (instead of the field enhancement g) as the quantity of interest, and implement the robust optimal design procedure. The obtained robust design with non-specified wavelength in the range [200 nm, 450 nm] is provided in Fig. 10(f) with mean $E = 6.34$ and standard deviation $\sigma = 0.59$.

5. Summary

In this paper, we implement robust design method under uncertainty for a robust design and adopt a classical robust model with the goal of minimizing both the mean and standard deviation of the cost function. Due to the consideration of the uncertainty in simulations, the robust optimization process may become computational expensive. Therefore, we propose an efficient numerical procedure for the robust design to reduce the computational cost. First, we implement global sensitivity analysis method to calculate the first order Sobol indices, based on which one can identity the "important" random variable. Following that, the dimension of the stochastic space may be reduced by considering the non-important ones as deterministic. To further reduce the computational cost, we then use generalized polynomial chaos expansion method to construct computationally cheaper surrogate models to approximate the full simulations. With the proper choice of the polynomials, the gPC expansion converges to the true function exponentially for smooth functions. The efficient robust design procedure is first illustrated using a simple one-dimensional example and then applied to metallic nanoparticles' design for the best enhancement of electric fields.

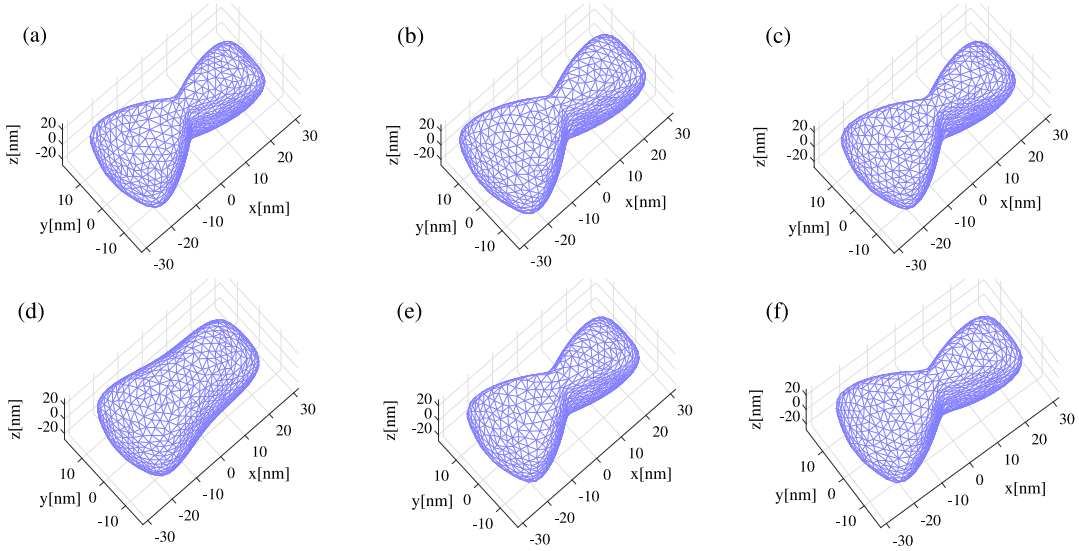

Fig. 10. The robust optimal design for silver nanoparticles to achieve high field enhancement with respect to different wavelength: (a) 250 nm, (b) 287 nm, (c) 320 nm, (d) 379 nm, (e) 435 nm, and (f) wavelength range [200 nm, 450 nm].

Acknowledgments

This research was sponsored by the Army Research Laboratory and was accomplished under Cooperative Agreement Number W911NF-12-2-0023 . The views and conclusions contained in this document are those of the authors and should not be interpreted as representing the official policies, either expressed or implied, of the Army Research Laboratory or the U.S. Government. The U.S. Government is authorized to reproduce and distribute reprints for Government purposes notwithstanding any copyright notation herein.

References

[1] J. Yelk, M. Sukharev, Optimal design of nanoplasmonic materials using genetic algorithms as a multiparameter optimization tool, J. Chem. Phys. 129 (6) (2008) 064706.
[2] V. Liu, D.A.B. Miller, S. Fan, Application of computational electromagnetics for nanophotonics design and discovery, Proc. IEEE 11 (2) (2013) 484–493.
[3] Z. Ruan, S. Fan, Design of subwavelength superscattering nanospheres, Appl. Phys. Lett. 98 (4) (2011) 043101.
[4] A. Tassadit, D. Macías, J.A. Sánchez-Gil, P.-M. Adam, R. Rodríguez-Oliveros, Metal nanostars: Stochastic optimization of resonant scattering properties, Superlattices Microstruct. 49 (3) (2011) 288–293.
[5] D. Macías, P.-M. Adam, V. Ruíz-Cortés, R. Rodríguez-Oliveros, J.A. Sánchez-Gil, Heuristic optimization for the design of plasmonic nanowires with specific resonant and scattering properties, Opt. Express 20 (2012) 13146–13163.
[6] T. Feichtner, O. Selig, M. Kiunke, B. Hecht, Evolutionary optimization of optical antennas, Phys. Rev. Lett. 109 (2012) 127701.
[7] C. Forestiere, Y. He, R. Wang, R.M. Kirby, L. Dal Negro, Inverse design of metal nanoparticles' morphology, ACS Photonics 3 (1) (2016) 68–78.
[8] J. Gielis, A generic geometric transformation that unifies a wide range of natural and abstract shapes, J. Am. J. Bot. 90 (2003) 333–338.
[9] R. Rodríguez-Oliveros, J.A. Sánchez-Gil, Localized surface-plasmon resonances on single and coupled nanoparticles through surface integral equations for flexible surfaces, Opt. Express 19 (13) (2011) 12208–12219.
[10] C. Forestiere, G. Iadarola, G. Rubinacci, A. Tamburrino, L. Dal Negro, G. Miano, Surface integral formulations for the design of plasmonic nanostructures, J. Opt. Soc. Am. A 29 (1) (2012) 2314–2327.
[11] D. Xiu, Fast numerical methods for robust optimal design, Eng. Optim. 40 (6) (2008) 489–504.
[12] P. Zhu, S. Zhang, W. Chen, Multi-point objective-oriented sequential sampling strategy for constrained robust design, Eng. Optim. 47 (3) (2015) 287–307.
[13] S. Zhang, P. Zhu, W. Chen, P. Arendt, Concurrent treatment of parametric uncertainty and metamodeling uncertainty in robust design, Struct. Multidiscip. Optim. 47 (2013) 63–76.
[14] N. Wiener, The homogeneous chaos, Amer. J. Math. 60 (4) (1938) 897–936.
[15] D. Xiu, G.E. Karniadakis, The Wiener-Askey polynomial chaos for stochastic differential equations, SIAM J. Sci. Comput. 24 (2) (2002) 619–644.

[16] D. Xiu, Numerical Methods for Stochastic Computations: A Spectral Method Approach, Princeton University Press, New Jersey, 2010.
[17] D. Xiu, Efficient collocational approach for parametric uncertainty analysis, Commun. Comput. Phys. 2 (2) (2007) 897–936.
[18] S. Marino, I.B. Hogue, C.J. Ray, D.E. Kirschner, A methodology for performing global uncertainty and sensitivity analysis in systems biology, J. Theoret. Biol. 254 (1) (2008) 178–196.
[19] I.M. Sobol, Sensitivity estimates for nonlinear mathematical models, Math. Model. Comput. Exp. 1 (1993) 407–414.
[20] I.M. Sobol, Global sensitivity indices for nonlinear mathematical models and their monte carlo estimates, Math. Comput. Simul. 55 (2001) 271–280.
[21] B. Sudret, Global sensitivity analysis using polynomial chaos expansions, Reliab. Eng. Syst. Saf. 93 (2008) 964–979.
[22] R. Cameron, W. Martin, The orthogonal development of nonlinear functionals in series of Fourier-Hermite functionals, Ann. of Math. 48 (2) (1947) 385–392.
[23] R.G. Ghanem, P.D. Spanos, Stochastic Finite Elements: A Spectral Approach, Springer, New York, 1991.
[24] F. Heiss, V. Winschel, Likelihood approximation by numerical integration on sparse grids, J. Econometrics 144 (2008) 62–80.
[25] V. Keshavarzzadeh, R.M. Kirby, A. Narayan, Numerical integration in multiple dimensions with designed quadrature, SIAM J. Sci. Comput. (2017) (submitted for publication).
[26] I.M. Sobol, S.S. Kucherenko, Global sensitivity indices for nonlinear mathematical models, Review, Wilmott Mag. 1 (2005) 56–61.